

Section 16: Magnetic properties of materials (continued)

Ferromagnetism

Ferromagnetism is the phenomenon of spontaneous magnetization – the magnetization exists in the ferromagnetic material in the absence of applied magnetic field. The best-known examples of ferromagnets are the transition metals Fe, Co, and Ni, but other elements and alloys involving transition or rare-earth elements also show ferromagnetism. Thus the rare-earth metals Gd, Dy, and the insulating transition metal oxide CrO₂ all become ferromagnetic under suitable circumstances.

Ferromagnetism involves the alignment of an appreciable fraction of the molecular magnetic moments in some favorable direction in the crystal. The fact that the phenomenon is restricted to transition and rare-earth elements indicates that it is related to the unfilled 3d and 4f shells in these substances.

Ferromagnetism appears only below a certain temperature, which is known as the *ferromagnetic transition temperature* or simply as the *Curie temperature*. This temperature depends on the substance, but its order of magnitude is about 1000°K for Fe, Co, Gd, Dy. It might be however much less. For example it is 70K for EuO and even less for EuS. Thus the ferromagnetic range often includes the whole of the usual temperature region.

Above the Curie temperature, the moments are oriented randomly, resulting in a zero net magnetization. In this region the substance is paramagnetic, and its susceptibility is given by

$$\chi = \frac{C}{T - T_C} \quad (1)$$

which is the *Curie-Weiss law*. The constant C is called the *Curie constant* and T_C is the *Curie temperature*.

The Curie-Weiss law can be derived using arguments proposed by Weiss. In the ferromagnetic materials the moments are magnetized spontaneously, which implies the presence of an internal field to produce this magnetization. Weiss assumed that this field is proportional to the magnetization, i.e.

$$\mathbf{B}_E = \lambda \mathbf{M} \quad (2)$$

where λ is the *Weiss constant*. Weiss called this field *the molecular field* and thought that this field results from all the molecules in the sample. In reality, the origin of this field is the *exchange interaction*. The exchange interaction is the consequence of the Pauli exclusion principle and the Coulomb interaction between electrons. Consider for example the system of two electrons. There are two possible arrangements for the spins of the electrons: either parallel or antiparallel. If they are parallel, the exclusion principle requires the electrons to remain far apart. If they are antiparallel, the electrons may come closer together and their wave functions overlap considerably. These two arrangements have different energies because, when the electrons are close together, the energy rises as a result of the large Coulomb repulsion. This is actually an explanation of the first Hund rule according to which the system of electrons tends to have a high possible spin, which is not forbidden by the Pauli principle. As we see from this example the electrostatic energy of an electron system depends on the relative orientation of the spins: the difference in energy defines the

exchange energy. The exchange interaction is short ranged. Therefore, only nearest neighbor atoms are responsible for producing the molecular field. The magnitude of the molecular (exchange) field is very large – of the order of 10^7G or 10^3T . It is not possible to produce such field in laboratories.

Weiss logic was as follows. Consider the paramagnetic phase: an applied magnetic field B_0 causes a finite magnetization. This in turn causes a finite exchange field B_E . If χ_p is the paramagnetic susceptibility, the induced magnetization is given by

$$\mathbf{M} = \chi_p (\mathbf{B}_0 + \mathbf{B}_E) = \chi_p (\mathbf{B}_0 + \lambda\mathbf{M}) \quad (3)$$

Note that the magnetization is equal to a constant susceptibility times a field only if the fractional alignment is small: this is where the assumption enters that the specimen is in the paramagnetic phase. Equation (3) should be considered as a self-consistent equation for the magnetization. It can be solved explicitly for the magnitude of the magnetization so that

$$M = \frac{\chi_p B_0}{1 - \chi_p \lambda} \quad (4)$$

We know that the paramagnetic susceptibility is given by the Curie law $\chi_p = C/T$, where C is the Curie constant. We then find for the susceptibility of the ferromagnetic material

$$\chi = \frac{M}{B_0} = \frac{C}{T - C\lambda} = \frac{C}{T - T_C} \quad (5)$$

The susceptibility (5) has a singularity at $T_C = C\lambda$. At this temperature (and below) there exists a spontaneous magnetization, because if χ is infinite so that we can have a finite M for zero B_0 . Using the expression we obtained earlier for C , i.e. $C = \frac{Np^2\mu_B^2}{3k_B}$, the Curie temperature is given by

$$T_C = \frac{N\lambda p^2 \mu_B^2}{3k_B}. \quad (6)$$

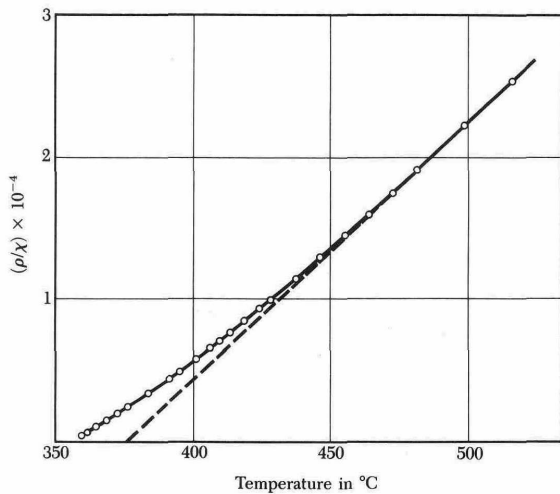


Fig.1 Reciprocal of the susceptibility per gram of nickel in the neighborhood of the Curie temperature (358°C). The dashed line is a linear extrapolation from high temperatures.

The Curie-Weiss law describes fairly well the observed susceptibility variation in the paramagnetic region above the Curie point (Fig.1). Only in the vicinity of the Curie temperature a notable deviations are observed. This due to the fact that strong fluctuations of the magnetic moments close to the phase transition temperature can not be described by the mean field theory which was used for deriving the Curie-Weiss law. Accurate calculations predict that

$$\chi \propto \frac{C}{(T-T_C)^{1.33}} \quad (7)$$

at temperatures very close to T_C .

We can also use the mean field approximation below the Curie temperature to find the magnetization as a function of temperature. We can proceed as before but instead of the Curie law which is valid for not too high magnetic fields and not too low temperatures we can use the complete Brillouin function. If we omit the applied magnetic field and replace B by the exchange field $B_E = \lambda M$ we find

$$M = NgJ\mu_B B_J \left(\frac{gJ\mu_B\lambda M}{kT} \right), \quad (8)$$

where $B_J(x)$ is the Brillouin function. This is a non-linear equation in M , which we can be solved numerically.

Now we shall see that solutions of this equation with nonzero M exist in the temperature range between 0 and T_C . To solve (8) we write it in terms of the reduced magnetization $m = NgJ\mu_B M$

and the reduced temperature $t = \frac{kT}{Ng^2\mu_B^2 J^2 \lambda}$, whence

$$m = B_J \left(\frac{m}{t} \right) \quad (9)$$

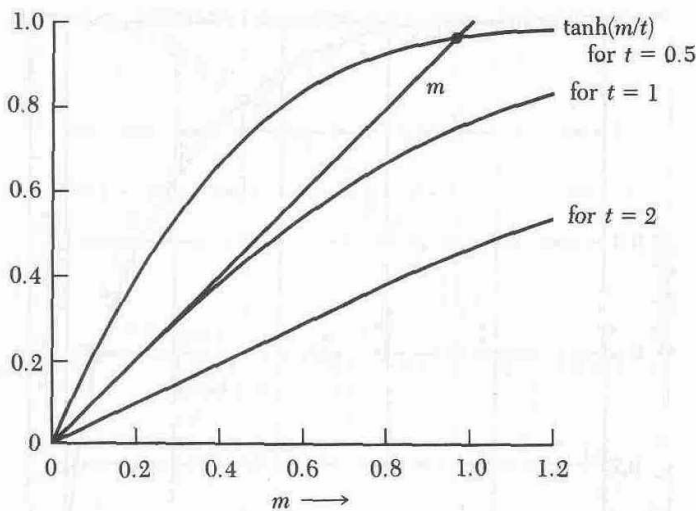


Fig.2 Graphical solution of Eq. (9) for the reduced magnetization m as a function of temperature. The left-hand side of Eq. (9) is plotted as a straight line m with unit slope. The right-hand side Eq. (9) is plotted vs. m for three different values of the reduced temperature $t = k_B T / N \mu_B^2 \lambda = T / T_C$. The three curves correspond to the temperatures $2T_C$, T_C , and $0.5T_C$. The curve for $t = 2$ intersects the straight line m only at $m = 0$, as appropriate for the paramagnetic region (there is no external applied magnetic field). The curve for $t = 1$ (or $T = T_C$) is tangent to the straight line m at the origin; this temperature marks the onset of ferromagnetism. The curve for $t = 0.5$ is in the ferromagnetic region and intersects the straight line m at about $m = 0.94N\mu_B$. As $t \rightarrow 0$ the intercept moves up to $m = 1$, so that all magnetic moments are lined up at absolute zero.

We then plot the right and left sides of this equation separately as functions of m , as in Fig. 2 which is plotted for $J=S=1/2$. The intercept of the two curves gives the value of m at the temperature of interest. The critical temperature is $t = 1$, or $T_C = N\mu_B^2 \lambda/k_B$.

The curves of M versus T obtained in this way reproduce roughly the features of the experimental results, as shown in Fig. 3 for nickel. As T increases the magnetization decreases smoothly to zero at $T = T_C$.

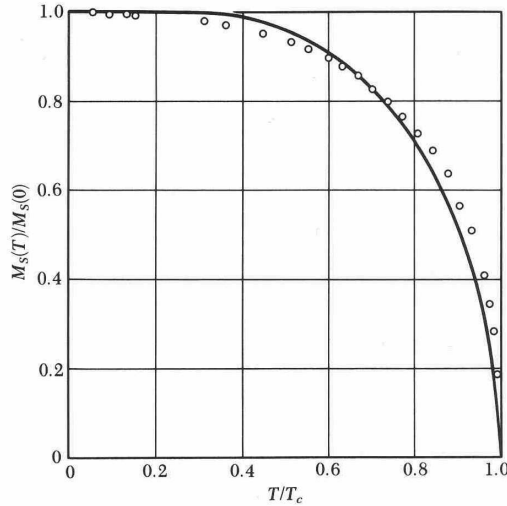


Fig.3 Saturation magnetization of nickel as a function of temperature, together with the theoretical curve for $S = 1/2$ on the mean field theory.

The mean field theory does not give a good description of the variation of M at low temperatures. The mean field theory predicts exponential convergence of the magnetization to the value at zero temperature. The experimental results show however a much more rapid dependence of ΔM on temperature at low temperatures, namely

$$\frac{\Delta M}{M} = AT^{3/2} \tag{10}$$

where A is some constant different for different metals. The result (10) finds a natural explanation in terms of spin wave theory.

Spin waves

In ferromagnetic materials the lowest energy of the system occurs when all spins are parallel to each other in the direction of magnetization. When one of the spins is tilted or disturbed, however, it begins to precess – due to the field from the other spins. Due to the exchange interaction between nearest neighbors the disturbance propagates as a wave through the system, as shown in Fig.4.

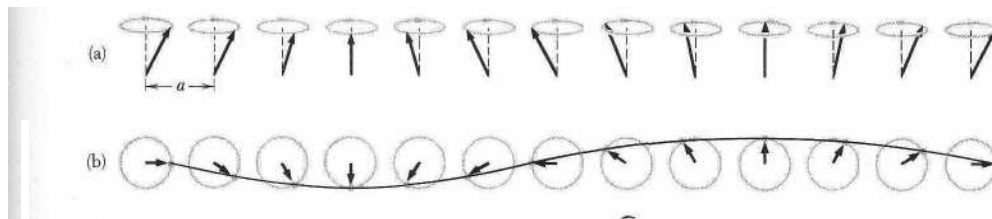


Fig.4 A spin wave on a line of spins, (a) The spins viewed in perspective, (b) Spins viewed from above, showing one wavelength. The wave is drawn through the ends of the spin vectors.

Spin waves are analogous to lattice waves. In lattice waves, atoms oscillate around their equilibrium positions, and their displacements are correlated through lattice forces. In spin waves, the spins precess around the equilibrium magnetization and their precessions are correlated through exchange forces.

Now we derive an expression for the frequency of the spin waves. We consider a linear chain of spins with nearest neighbor spins coupled by the Heisenberg interaction:

$$U = -2J \sum_{p=1}^N \mathbf{S}_p \cdot \mathbf{S}_{p+1} \quad (11)$$

where J is the exchange integral and \mathbf{S}_p is spin at site p . For simplicity we will use classical theory in which spin operators are replaced by classical vectors. According to (11) the interaction which involves the p -th spin is

$$-2J \mathbf{S}_p \cdot (\mathbf{S}_{p-1} + \mathbf{S}_{p+1}). \quad (12)$$

This interaction can be rewritten as $-\boldsymbol{\mu}_p \cdot \mathbf{B}_p$, where $\boldsymbol{\mu}_p = -g\mu_B \mathbf{S}_p$ is the magnetic moment associated with spin \mathbf{S}_p and \mathbf{B}_p is an effective magnetic field or exchange field acting on this moment due to nearest neighbor spins:

$$\mathbf{B}_p = -\frac{2J}{g\mu_B} (\mathbf{S}_{p-1} + \mathbf{S}_{p+1}). \quad (13)$$

According to classical mechanics the rate of change of the angular momentum $\hbar \mathbf{S}_p$ is equal to the torque $\boldsymbol{\mu}_p \times \mathbf{B}_p$ which acts on the spin, i.e.

$$\frac{\hbar d\mathbf{S}_p}{dt} = \boldsymbol{\mu}_p \times \mathbf{B}_p, \quad (14)$$

or

$$\frac{d\mathbf{S}_p}{dt} = -\left(\frac{g\mu_B}{\hbar} \mathbf{S}_p\right) \times \left[-\frac{2J}{g\mu_B} (\mathbf{S}_{p-1} + \mathbf{S}_{p+1})\right] = \frac{2J}{\hbar} \mathbf{S}_p \times (\mathbf{S}_{p-1} + \mathbf{S}_{p+1}), \quad (15)$$

Normally the amplitude of excitation is very small, so that $S_p^z \approx S$ and $S_p^x, S_p^y \ll S$. This allows to linearize Eqs.(15):

$$\begin{aligned} \frac{dS_p^x}{dt} &= \frac{2JS}{\hbar} (2S_p^y - S_{p-1}^y - S_{p+1}^y) \\ \frac{dS_p^y}{dt} &= \frac{2JS}{\hbar} (2S_p^x - S_{p-1}^x - S_{p+1}^x), \\ \frac{dS_p^z}{dt} &= 0 \end{aligned} \quad (16)$$

By analogy with the problem of lattice vibrations we look for traveling wave solutions of the form

$$\begin{aligned} S_p^x &= u \exp[i(pka - \omega t)] \\ S_p^y &= v \exp[i(pka - \omega t)] \end{aligned} \quad (17)$$

where u and v are constants and a is the lattice constant. By substitution into (16) we obtain

$$\begin{aligned} -i\omega u &= \frac{2JS}{\hbar} (2 - e^{-ika} - e^{ika}) v = \frac{4JS}{\hbar} (1 - \cos ka) v \\ -i\omega v &= -\frac{2JS}{\hbar} (2 - e^{-ika} - e^{ika}) u = -\frac{4JS}{\hbar} (1 - \cos ka) u \end{aligned} \quad (18)$$

These equations have a solution if the determinant of coefficients is equal to zero, i.e.

$$\begin{vmatrix} i\omega & \frac{4JS}{\hbar} (1 - \cos ka) \\ -\frac{4JS}{\hbar} (1 - \cos ka) & i\omega \end{vmatrix} = 0. \quad (19)$$

This leads to the dispersion relation

$$\omega = \frac{4JS}{\hbar} (1 - \cos ka), \quad (20)$$

which is plotted in Fig. 5.

With this solution we find that $v = -iu$. This corresponds to circular precession of each spin about the z axis. We can see this by taking real parts of (17) with v set to $-iu$. Then

$$\begin{aligned} S_p^x &= u \cos(pka - \omega t) \\ S_p^y &= u \sin(pka - \omega t) \end{aligned} \quad (21)$$

The corresponding spin wave is shown in Fig.4.

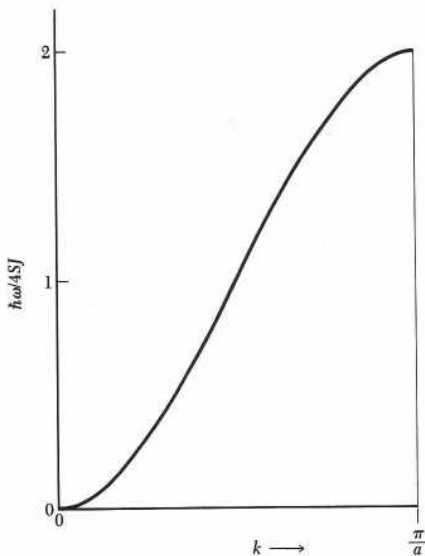


Fig.5 Dispersion relation for magnons in a ferromagnet in one dimension with nearest-neighbor interactions.

In a long wave limit, $ka \ll 1$, we find

$$\omega \simeq \frac{2JSa^2}{\hbar} k^2. \quad (22)$$

The frequency is proportional to k^2 . Note that in the same limit the phonon frequency is proportional to k .

Generalization to a three dimensional cubic lattice with nearest-neighbor interaction results in

$$\omega = \frac{4JS}{\hbar} \left[z - \sum_{\delta} \cos(\mathbf{k} \cdot \delta) \right], \quad (23)$$

where the summation is over the z vectors denoted by δ which join the central atom to its nearest neighbors. In the limit $ka \ll 1$ we find for all three cubic lattices

$$\omega \simeq \frac{2JSa^2}{\hbar} k^2, \quad (24)$$

which is the same result as (22).

Thermal excitation of magnons

Spin waves can be quantized in a similar way as phonons. A quantized spin wave is called *magnon*. The energy of a magnon mode of frequency $\omega_{\mathbf{k}}$ with $n_{\mathbf{k}}$ magnons is given by

$$E_{\mathbf{k}} = \hbar \omega_{\mathbf{k}} (n_{\mathbf{k}} + 1/2). \quad (25)$$

In thermal equilibrium the average number of magnons excited in the mode \mathbf{k} is given by the Planck distribution

$$\langle n_{\mathbf{k}} \rangle = \frac{1}{\exp(\hbar \omega_{\mathbf{k}} / k_B T) - 1}. \quad (26)$$

The total number of magnons excited at temperature T is

$$\sum_{\mathbf{k}} n_{\mathbf{k}} = \int d\omega D(\omega) \langle n(\omega) \rangle, \quad (27)$$

where $D(\omega)$ is the number of magnon modes per unit frequency range. The integral is taken over allowed values of \mathbf{k} lying in the first Brillouin zone. At sufficiently low temperatures we may carry the integral between 0 and ∞ because $\langle n(\omega) \rangle \rightarrow 0$ exponentially as $\omega \rightarrow \infty$.

Magnons have a single polarization for each value of \mathbf{k} . In three dimensions the number of modes of wavevector less than k is $(1/2\pi)^3 (4\pi k^3/3)$ per unit volume, whence the number of magnons $D(\omega)d\omega$ with frequency in $d\omega$ at ω is $(1/2\pi)^3 (4\pi k^2)(dk/d\omega)d\omega$. In the longwave limit (24) (we can use a longwave limit here because at low temperatures only magnons which have low frequency and therefore small wavevector are thermally excited), we find

$$\frac{d\omega}{dk} = \frac{4JSa^2}{\hbar} k = 2 \left(\frac{2JSa^2}{\hbar} \right)^{1/2} \omega^{1/2}. \quad (28)$$

Therefore the density of magnon modes is

$$D(\omega) = \frac{1}{4\pi^2} \left(\frac{\hbar}{2JSa^2} \right)^{3/2} \omega^{1/2}. \quad (29)$$

Thus the total number of magnons is

$$\sum_{\mathbf{k}} n_{\mathbf{k}} = \frac{1}{4\pi^2} \left(\frac{\hbar}{2JSa^2} \right)^{3/2} \int_0^{\infty} \frac{\omega^{1/2} d\omega}{\exp(\hbar\omega/k_B T) - 1} = \frac{1}{4\pi^2} \left(\frac{k_B T}{2JSa^2} \right)^{3/2} \int_0^{\infty} \frac{x^{1/2} dx}{e^x - 1}. \quad (30)$$

The definite integral is equal to $(0.0587)(4\pi^2)$.

The number of N of atoms per unit volume is Q/a^3 , where $Q=1,2,4$ for sc, bcc and fcc lattices. Since the excitation of a magnon corresponds to the reversal of one spin, $\sum_{\mathbf{k}} n_{\mathbf{k}} / NS$ is equal to the fractional change of magnetization $\Delta M / M$, whence

$$\frac{\Delta M}{M} = \frac{0.0587}{SQ} \left(\frac{k_B T}{2JS} \right)^{3/2}. \quad (31)$$

The result is the *Bloch $T^{3/2}$ law* which is confirmed experimentally.

Ferrimagnetism

The Heisenberg model (11) leads to ferromagnetism, if the constant J is positive. The parallel-aligned state will then have a lower energy than the antiparallel state. The negative constant in Eq.(11) leads to antiferromagnetism or ferrimagnetism. Figure 6b illustrates an *antiferromagnetic* arrangement, in which the dipoles have equal moments, but adjacent dipoles point in opposite directions. Thus the moments balance each other, resulting in a zero net magnetization. Another type of arrangement commonly encountered is the *ferrimagnetic* pattern shown in Fig.6c. Neighboring dipoles point in opposite directions, but since in this case the moments are unequal, they do not balance each other completely, and there is a finite net magnetization. Now we discuss the ferrimagnetic arrangement.

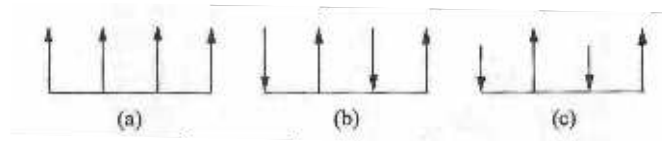


Fig.6 Magnetic arrangements: (a) ferromagnetic, (b) antiferromagnetic, (c) ferrimagnetic.

The most familiar example of a ferrimagnetic material is magnetite, Fe_3O_4 . More explicitly, the chemical composition is $\text{FeO} \cdot \text{Fe}_2\text{O}_3$, showing that there are two types of iron ions: ferrous (doubly charged), and ferric (triply charged). The compound crystallizes in the spinel structure. The unit cell contains 56 ions, 24 of which are iron ions and the remainder oxygen. The magnetic moments are

located on the iron ions. If we study the unit cell closely, we find that the Fe ions are located in either of two different coordinate environments: A tetrahedral one, in which the Fe ion is surrounded by 4 oxygen ions, and an octahedral one, in which it is surrounded by 6 oxygen ions. Of the 16 ferric ions in the unit cell, 8 are in one type of position and 8 are in the other. Furthermore, the tetrahedral structure has moments oriented opposite to those of the octahedral one, resulting in a complete cancellation of the contribution of the ferric ions. The net moment therefore arises entirely from the 8 ferrous ions which occupy octahedral sites. Each of these ions has six 3d electrons, whose spin orientations are $\uparrow\uparrow\uparrow\uparrow\downarrow$. Hence each ion carries a moment equal to 4 Bohr magneton.

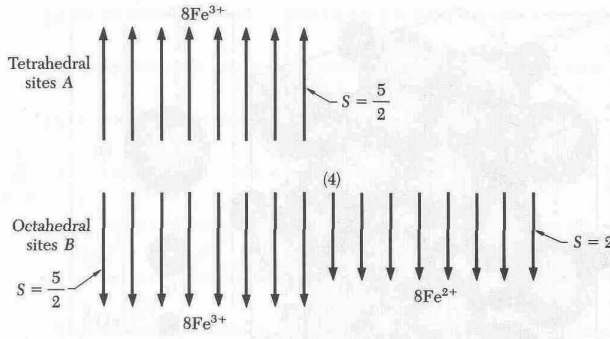


Fig.7 Spin arrangements in magnetite, $\text{FeO}\cdot\text{Fe}_2\text{O}_3$, showing how the moments of the Fe^{3+} ions cancel out, leaving only the moments of the Fe^{2+} ions.

There are many other materials which have ferrimagnetic properties. An important class of magnetic oxides is known as ferrites. The usual chemical formula of a ferrite is $\text{MO}\cdot\text{Fe}_2\text{O}_3$, where M is a divalent cation, often Zn, Cd, Fe, Ni, Cu, Co, or Mg.

Now we calculate the Curie temperature and susceptibility of ferromagnets using the mean field theory. We assume that the lattice consists of two types of ions which have different magnetic moments and positions at sites A and B. We assume that there is an antiparallel interaction between the A and B sites so that $\mathbf{B}_A = -\lambda\mathbf{M}_B$ and $\mathbf{B}_B = -\lambda\mathbf{M}_A$, where λ is positive. We define Curie constants C_A and C_B for the ions on the A and B sites. Within the mean field approximation we obtain

$$\begin{aligned} \mathbf{M}_A &= \frac{C_A}{T}(B_0 - \lambda\mathbf{M}_B) \\ \mathbf{M}_B &= \frac{C_B}{T}(B_0 - \lambda\mathbf{M}_A) \end{aligned} \quad (32)$$

where B_0 is the applied field. These equations have a nonzero solution for M_A and M_B in zero applied field if

$$\begin{vmatrix} T & \lambda C_A \\ \lambda C_B & T \end{vmatrix} = 0, \quad (33)$$

so that the ferrimagnetic Curie temperature is given by

$$T_C = \lambda\sqrt{C_A C_B}. \quad (34)$$

We solve (34) for M_A and M_B to obtain the susceptibility at $T > T_C$:

$$\chi = \frac{M_A + M_B}{B_0} = \frac{(C_A + C_B)T - 2\lambda C_A C_B}{T^2 - T_C^2}. \quad (35)$$

This result is more complicated than that for ferromagnets. Experimental values for Fe_3O_4 are plotted in Fig.8. The curvature of the plot of $1/\chi$ versus T is a characteristic feature of a ferrimagnet.

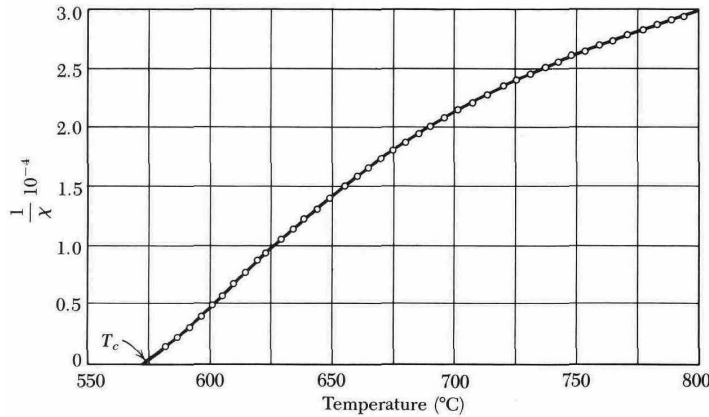


Fig.8 Reciprocal susceptibility of magnetite.

Many ferromagnets exhibit a very interesting behavior of the saturation magnetization versus temperature which is shown in Fig.9.

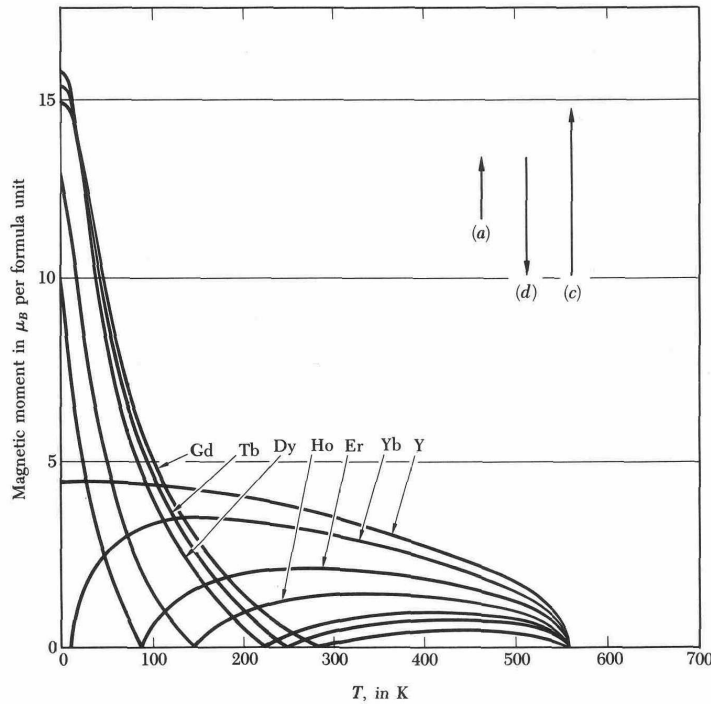


Fig.9 Experimental values of the saturation magnetization versus temperature of various iron garnets. The formula unit is $\text{M}_3\text{Fe}_5\text{O}_{12}$, where M is a trivalent metal ion. The temperature at which the magnetization crosses zero is called the *compensation temperature*; here the magnetization of the M sublattice is equal and opposite to the net magnetization of the ferric ion sublattices. Per formula unit there are 3 Fe^{3+} ions on tetrahedral sites d; 2 Fe^{3+} ions on octahedral sites a; and 3 M^{3+} ions on sites denoted by c. The ferric ions contribute $(3 - 2)5\mu_B = 5\mu_B$ per formula unit. The ferric ion coupling is strong and determines the Curie temperature. If the M^{3+} ions are rare-earth ions they are magnetized opposite to the resultant of the Fe^{3+} ions. The M^{3+} contribution drops rapidly with increasing temperature because the M-Fe coupling is weak.

Antiferromagnetism

An antiferromagnet is a special case of a ferrimagnet for which both sublattices A and B have equal saturation magnetizations. In an antiferromagnet the spins are ordered in an antiparallel arrangement with zero net moment at temperatures below the ordering temperature which is called the *Néel temperature*. Thus $C_A = C_B$ in (34), and

$$T_N = \lambda C, \quad (36)$$

where C refers to a single sublattice. This expression is identical to that we obtained earlier for ferromagnetic materials. However, in this case the susceptibility in the paramagnetic region behaves in a different fashion. For $T > T_N$ we obtain from (35)

$$\chi = \frac{2CT - 2\lambda C^2}{T^2 - (\lambda C)^2} = \frac{2C}{T + T_N}. \quad (37)$$

At and above the Néel temperature the susceptibility is nearly independent of the direction of the field relative to the spin axis. However, below the Néel temperature the susceptibility of antiferromagnets depends strongly on the orientation of magnetic field. There are two situations: with the applied magnetic field perpendicular to the axis of the spins; and with the field parallel to the axis of the spins.

For B_0 perpendicular to the axis of the spins we can calculate the susceptibility from the energy density which is

$$U = \lambda \mathbf{M}_A \cdot \mathbf{M}_B - \mathbf{B}_0 \cdot (\mathbf{M}_A + \mathbf{M}_B) \cong -\lambda M^2 \left(1 - \frac{1}{2} (2\varphi)^2 \right) - 2B_0 M \varphi, \quad (38)$$

where $M = |\mathbf{M}_A| = |\mathbf{M}_B|$, and 2φ is the angle the spins make with each other (Fig.10a).

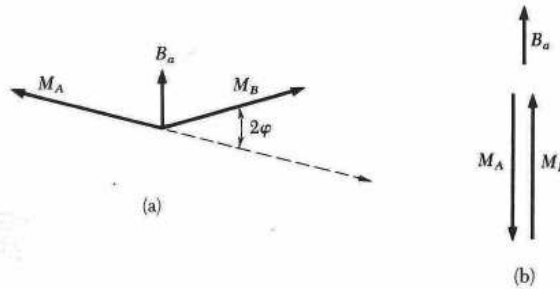


Fig.10 Magnetic susceptibility parallel and perpendicular to the tetragonal axis.

The energy is a minimum when

$$\frac{dU}{d\varphi} = 0 = 4\lambda M^2 \varphi - 2B_0 M, \quad (39)$$

$$\varphi = \frac{B_0}{2\lambda M}$$

so that

$$\chi_{\perp} = \frac{2M\phi}{B_0} = \frac{1}{\lambda}. \quad (40)$$

In the parallel orientation (Fig.10b) the magnetic energy is not changed if the spins make equal angles with the field. Thus the susceptibility at $T=0\text{K}$ is zero:

$$\chi_{\parallel} = 0. \quad (41)$$

The parallel susceptibility increases smoothly with temperature up to T_N . The χ_{\perp} and χ_{\parallel} for MnF_2 are shown in Fig.11.

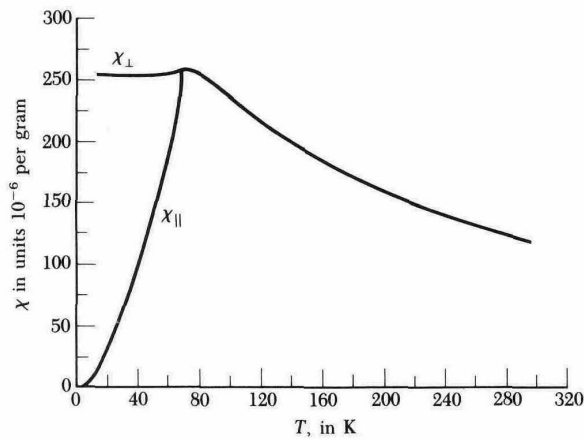


Fig.11 Magnetic susceptibility of manganese fluoride, MnF_2 , parallel and perpendicular to the tetragonal axis.

a uniformly magnetized state. There are four types of energy which contribute to the total energy of the material.

1. Exchange energy

This is the energy which is responsible for ferromagnetism of magnetic materials. The exchange coupling between nearest neighbors is significant and results in parallel alignment of the magnetizations in ferromagnetic materials. In a classical view of the Heisenberg representation the exchange coupling between nearest spins can be written as follows:

$$E_{ex} = -2JS_i\mathbf{S}_j = -2JS_iS_j \cos \theta \quad (42)$$

where J is the exchange integral and \mathbf{S}_i and \mathbf{S}_j are two neighboring spins. The sign of the exchange integral determines whether we have ferromagnetic or antiferromagnetic coupling. For ferromagnetic materials J is positive.

If there were no other type of energy to consider, then obviously all magnetic materials would be magnetized to saturation all the time. In the presence of other interactions the exchange coupling tries to ensure that the angle between them is as small as possible. Because the exchange interaction is strong, we may assume that the angle between two spins $\delta\phi$ is small. In this case

$$E_{ex} \approx 2JS^2 \frac{\delta\phi^2}{2} + const \quad (43)$$

where we assumed that $S=S_i=S_j$. The constant is independent of angle and can be put equal to zero because we can measure all the energies relative to this constant.

Now consider a material with a simple cubic structure with a lattice constant a . Let x , y and z to be the Cartesian axes and assume for simplicity that the magnetic moments are parallel everywhere to yz plane. The orientation of magnetic moments varies with x so that ϕ is the angle between the magnetic moment and the y -axis and $\delta\phi$ is the angle between neighboring moments. Because $\delta\phi$ is normally very small we can regard it as a continuous function of x and therefore

$$\delta\phi \approx a \frac{d\phi}{dx} \quad (44)$$

Therefore the exchange energy per unit volume is

$$E_{ex} \approx \frac{JS^2 a^2}{V} \left(\frac{d\phi}{dx} \right)^2 = A \left(\frac{d\phi}{dx} \right)^2 \quad (45)$$

where A is the *exchange stiffness constant*, which can serve as a characteristic of a ferromagnetic material. A typical value for the exchange stiffness constant in ferromagnetic metals is 10^{-6} erg/cm.

2. Magnetostatic energy

Now we come to the question of why a magnetic material should not always be uniformly magnetized like as is shown in Fig.13a. The state of uniform magnetization has the lowest possible exchange energy, since all adjacent spins are parallel to each other. However, the exchange energy is not the only type of energy that a magnetic material has. This state costs a large amount of magnetostatic energy. The magnetization generates north poles on the top surface and south poles

on the bottom surface. These poles act as the source of magnetic field. They can be thought as “magnetic” charges. These poles produce a magnetic field which is shown in Fig.13a.

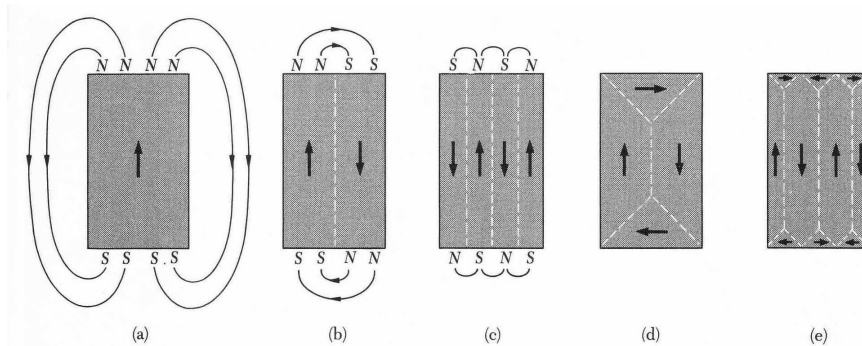


Fig. 13 (a) A ferromagnet in a state of uniform magnetization; (b) A ferromagnet divided into two ferromagnetic domains. Note that field lines are now confined primarily to end regions. (c) Subdividing into four domains (d) Domain closure – further reduction of the magnetostatic energy (e) Small edge domains due to magnetoelastic energy.

In addition to the field outside the specimen there is also field inside the specimen which is not shown here. This field is in the opposite direction to the magnetization. This field tries to demagnetize the specimen and is called the *demagnetization field* \mathbf{B}_d . The respective energy is called magnetostatic or demagnetization energy. The density of this energy is given by

$$E_m = -\frac{1}{2}\mathbf{M}\mathbf{B}_d \quad (46)$$

The value of \mathbf{B}_d depends on the shape of the specimen, and is usually written as

$$B_{dx} = -N_x M_x \quad B_{dy} = -N_y M_y \quad B_{dz} = -N_z M_z \quad (47)$$

where N_x , N_y , and N_z are the *demagnetization factors*. This factor, which is large for a flat sample and small for an elongated sample, is equal to unity for a sample in the shape of a thin, flat disc normal to the field. The magnetostatic energy is of the order of 10^7 erg/cm³. The fields which are produced by the uniformly magnetized sample are huge and the magnetic system will try to reduce them.

What happens if the specimen is subdivided into two domains (Fig.13b). In this case the top surface carries north poles on the left and south poles on the right, and the bottom surface carries south poles on the left and north poles on the right. The demagnetizing field does not extend from the top surface to the bottom, but it is confined to the region near the two ends of the specimen. As the specimen is further subdivided into smaller domains, the effect of the demagnetizing field becomes even smaller (Fig.13c,d).

What happens with the exchange energy in a state where the magnetic sample is subdivided into domains. You see that this state does not correspond to a minimum of the exchange energy. The exchange energy is minimized for uniformly magnetized material. However, the exchange interaction is quite short-ranged. Therefore, only spins near domain boundaries will experience unfavorable exchange interactions with the nearby spins in the neighboring misaligned domain. On the contrary, the dipolar interaction is long-ranged. Therefore, all the spins in the sample are

involved in the magnetic dipolar interactions. And therefore, subdivision into domains is energetically favorable.

We see therefore that the main reason for the subdivision into domains is magnetostatic energy. However, it is not the whole story.

3. Anisotropy energy

We can ask ourselves, what is wrong with a configuration in which magnetization is gradually rotates? If the magnetization rotates very slowly, it has very little exchange energy. It appears however that this configuration does not normally exist. There is usually a structure consisting of uniformly magnetized domains, separated by narrow boundaries. The reason is that there is another kind of energy which is called magnetic anisotropy. It arises from the crystalline nature of most magnetic materials. That is why it is often called *magnetocrystalline anisotropy*.

Due to crystalline structure of most magnetic materials the directions in which the magnetization is allowed to point are restricted. The magnetization prefers to be parallel to certain crystallographic directions. In this sense crystals are anisotropic. If the magnetization deviates from these directions there is an extra cost in energy which is called the *anisotropy energy*.

The origin of magnetocrystalline anisotropy is spin-orbit interaction. The magnetization of the crystal sees the crystal lattice through orbital overlap of the electrons: the spin interacts with the orbital motion by means of the spin-orbit coupling.

Magnetic anisotropy reflects the symmetry of the lattice. In cubic monocrystals the anisotropy energy can be expressed as

$$E_a = K_1(\alpha_1^2\alpha_2^2 + \alpha_1^2\alpha_3^2 + \alpha_2^2\alpha_3^2) + K_2\alpha_1^2\alpha_2^2\alpha_3^2 \quad (48)$$

where K_1 is the first order and K_2 is the second order anisotropy constants and $\alpha_1, \alpha_2, \alpha_3$ are the direction cosines referred to the cube axes. This form of the expression comes from symmetry considerations. It can be shown that this expression is invariant under all transformation of the cubic symmetry. If constants K_1 and K_2 are positive (of the order of 10^5 erg/cm³) which is the case for Fe and Ni, the anisotropy energy has a minimum when the magnetization is aligned along (100) direction. This is the case for example for iron. (100) is called the easy axis because the magnetization can be very easily saturated if the magnetic field is applied in this direction.

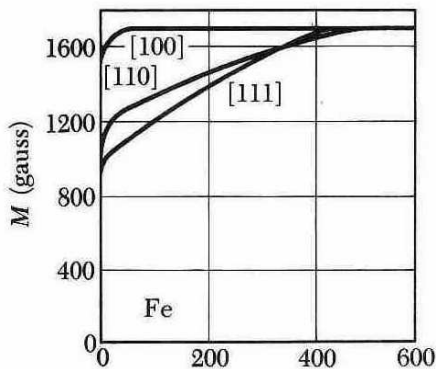


Fig.14 Magnetization curves for single crystal of iron. From the curves for iron we see that the [100] directions are easy directions of magnetization and the [110] and [111] directions are hard directions.

This can be seen from Fig.14, where the magnetization of iron as a function of the magnetic field is shown. If the magnetic field is applied along (100) direction the magnetization very rapidly reaches the saturation. On the contrary, if the magnetic field is applied along (110) or (111) directions the magnetization reaches the saturation only in a relatively high fields. That is why (110) and (111) axes are called the hard axes of magnetization.

In uniaxial crystals which have tetragonal, hexagonal and trigonal symmetries, the anisotropy per unit volume can be written as

$$E_a = K_1 \sin^2 \theta + K_2 \sin^4 \theta \quad (49)$$

where θ is the angle between the magnetization and the main symmetry axis. If $K_1 > 0$ the magnetization prefers to be parallel to the symmetry axis. In this case this axis is called the easy axis. If $K_1 < 0$ it prefers to be perpendicular to the symmetry axis. In this case it is called the hard axis.

Now let us return to the domain structures. The domain configuration with gradually rotating magnetization is not possible because it would cost too much anisotropy energy because in a large part of the specimen the magnetization is not parallel to an easy direction. The magnetization prefers certain direction in crystals and can not rotate gradually over long distances. In order to reduce the anisotropy energy the domains have to have abrupt boundaries.

This configuration would have very little exchange, magnetostatic and anisotropy energy if this is a cubic crystal and this is (100) direction. It turns out however that simple structures with large domains do not usually occur. We usually have a much larger number of much smaller domains. In order to understand why it happens we have to consider the magnetoelastic energy.

4. Magnetoelastic energy

When the magnetization of the material is changed, there is a slight change in its dimensions, generally of the order of 10^{-5} or less. Some materials expand in the direction of the magnetization, others, for example nickel, contract. This effect is called *magnetostriction*. The materials which expand are said to have positive magnetostriction, the materials which contract are said to have negative magnetostriction. Therefore, the change in the magnetization of the material results in elastic distortions. The energy associated with these distortions is called the *magnetoelastic energy*. The larger the domains are, the more elastic energy is needed. It is therefore favorable to form smaller domains at the domain boundaries of larger domains (Fig.13e). This costs less elastic energy to hold the domains together.

Domain walls

In order to complete the picture about domain structures we should consider the boundary between neighboring domains which called domain walls. Qualitatively it is clear that the width of the domain wall is determined by the balance between the exchange energy and the anisotropy energy. If the exchange is very strong and anisotropy is small we can expect that the width of the domain wall is large. On the contrary, in the case when the exchange energy is small and anisotropy is large the width of the domain wall should be small.

In order to calculate the width of the domain wall we assume that we have a 180° domain wall as is shown in Fig.15. That means that this wall separates two domains magnetized in opposite directions – the magnetization rotates by 180 degrees.

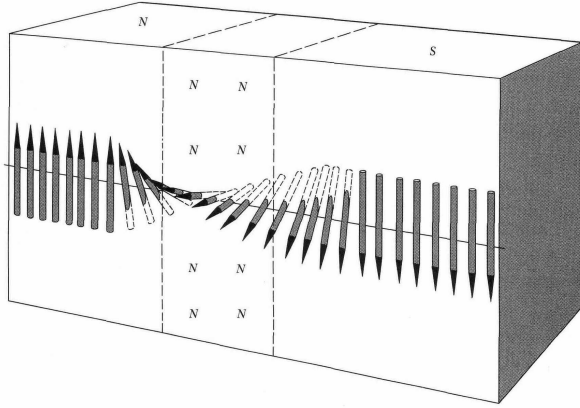


Fig.15 The structure of the Bloch wall separating domains.

The exchange energy per unit area of the domain wall is

$$E_{ex} = A \left(\frac{d\phi}{dx} \right)^2 \delta, \quad (50)$$

where δ is the domain wall width. For the case considered we can use estimate

$$\left(\frac{d\phi}{dx} \right)^2 = \frac{\pi^2}{\delta^2}, \quad (51)$$

so that

$$E_{ex} = \frac{A\pi^2}{\delta}. \quad (52)$$

For the anisotropy energy per unit area we take a rough estimate

$$E_a = K\delta \quad (53)$$

where K is anisotropy constant. The total energy of the domain wall per unit area is

$$E = E_{ex} + E_a = \frac{A\pi^2}{\delta} + K\delta. \quad (54)$$

In the equilibrium we have

$$\frac{dE}{d\delta} = 0, \quad (55)$$

which gives

$$\delta = \pi\sqrt{A/K} \quad (56)$$

and

$$E = 2\pi\sqrt{AK} . \quad (57)$$

For typical values $A \sim 10^{-6}$ erg/cm and $K \sim 10^5$ erg/cm³ we have $\delta \sim 100$ nm. The typical size of the domains is 1-100 μ m and therefore the width of the domain walls is much smaller. That is why the domain structure consists of uniformly magnetized domains separated by narrow boundaries.

The effect of applied field and domain wall motion

Now we consider qualitatively the effect of applied field on the domain structure. The applied magnetic field tends to align the magnetization parallel to the field. There are two ways to reduce the energy. First, the domain wall can move, thereby increasing the volume of the domain whose energy is lower and decreasing the volume of the other. Second, the magnetization direction of the two domains can change. Both these processes, i.e. the domain wall motion and the magnetization rotation, can occur in practice.

The position of the domain walls depends on the demagnetizing energy. When the external field is applied, the magnetic field inside the specimen is the sum of the demagnetizing field and the applied field. The domain walls will therefore generally move to new positions. On the other hand, the magnetization orientations are determined mainly by the anisotropy, which resists the rotation of the magnetization. In general therefore domain wall motion tends to occur in small applied fields, and the magnetization rotation only begins as the field is large enough.

Domain walls move reversibly in very small magnetic fields. In other words, the domain walls are displaced by a small amount when the field is applied, but if the field is removed, they return to their original positions. In larger fields the domain wall motion becomes irreversible - the walls do not return to their original positions when the field is removed. The main reason of that is that the domain wall energy is not a constant but varies in an irregular manner because of imperfections of the specimen. These imperfections are dislocations, grain boundaries, voids, lattice distortions, impurities. When the aligning field is removed, these defects may prevent the domain walls from returning to their original configuration. It then becomes necessary to apply a rather strong field in the opposite direction to restore the unmagnetized configuration. This is the origin of the *hysteresis* in ferromagnetic materials.